Weakly Bonded Lewis Base Adducts of Plumbocene and Stannocene: A Synthetic and Calculational Study

David R. Armstrong,[†] Michael A. Beswick,[‡] Natalie L. Cromhout,[‡] Christopher N. Harmer,[‡] David Moncrieff,[§] Christopher A. Russell,[‡] Paul R. Raithby,[‡] Alexander Steiner,[‡] Andrew E. H. Wheatley,[‡] and Dominic S. Wright*[,‡]

Department of Pure and Applied Chemistry, University of Strathclyde, 295 Cathedral Street, Glasgow G1 1XL, U.K., Department of Chemistry, University of Cambridge, Lensfield Road, Cambridge CB2 1EW, U.K., and Supercomputer Computations Research Institute, Florida State University, Tallahassee, Florida 32306-4052

Received February 4, 1998

The coordination of [(η-Cp)$_2$Pb] and [(η-Cp)$_2$Sn] by bidentate Lewis-base ligands gives the first examples of adducts of neutral p-block metallocenes. Ab initio MO calculations of [(η-Cp)$_2$Pb·TMEDA] (**1**) (TMEDA = (Me$_2$NCH$_2$)$_2$), [Cp$_2$Pb·4,4′-Me$_2$bipy] (**2**) (4,4′-Me$_2$bipy = 4,4′-dimethylbipyridine), and the new complex [(η-Cp)$_2$Sn·TMEDA] (**3**) confirm that despite the presence of longer Pb−N and Sn−N bonds in the solid-state structures of the TMEDA adducts, the association of TMEDA with the metallocenes is more favorable than with 4,4′-Me$_2$bipy. This finding is a consequence of the greater reorganization energy of 4,4′-Me$_2$bipy compared to TMEDA. The low association energies of these species can be rationalized in terms of metal lone pair/ligand lone pair repulsion.

Introduction

Although the parent main-group metallocenes (containing unsubstituted cyclopentadienide (Cp = C$_5$H$_5$) ligands) have been known for as long as their transition-metal counterparts, the bonding and reactivities of these species have been studied far less extensively.[1] What is apparent from structural and calculational investigations performed thus far is that, owing to minimal d orbital involvement and to the more varied (ionic and/or covalent) character of the metal−ligand interactions, main-group metallocenes exhibit greater structural variety and have less restricted electronic requirements.[1,2] The simplest group 14 metallocenes, [(η-Cp)$_2$E] (E = Sn, Pb), have mononuclear 14e angular sandwich structures in the gas phase,[2h,i] which is in marked contrast to the linear arrangements observed for the (formally) 12e sandwich structures of [(η-Cp)$_2$Mg][2e] and [(η-Cp)$_2$Li]$^-$.[2f] Ab initio calculations of [(η-Cp)$_2$Ge] suggest that the adoption of the bent (rather than linear) arrangement for the group 14 complexes arises from the associated admixing of the metal p_x atomic orbital with the initially antibonding lone-pair orbital, resulting in net stabilization of the lone pair.[3] However, the observation of two different bent conformers of stannocene in the solid state[2g] and the adoption of a polymeric strand structure for crystalline orthorhombic plumbocene[2i] suggests that the stabilization effect of admixing for the heavier group 14 elements is far less profound than was assumed and that the lone-pair orbitals in these species have largely s character and minimal stereochemical activity. More recent ab initio calculations of [(η-Cp)$_2$E] (E = Sn, Pb) confirm these conclusions by illustrating that the energy difference between the bent and linear geometries and the stabilization effect on the lone pair decreases on going from Sn to Pb.[4] The fact that the lone pairs are more core-like in these complexes is also apparent from their inability to form adducts with Lewis acids (such as BF$_3$[5]) and, in particular, from the formation of species such as [(η-Cp)$_3$E]$^-$ in which the metals of [(η-Cp)$_2$E] accept electron density from a Cp$^-$ anion.[6]

In a recent communication, we showed that simple Lewis-base adducts of [(η-Cp)$_2$Pb] are readily prepared by dissolving plumbocene in toluene-containing biden-

[†] University of Strathclyde.
[‡] University of Cambridge.
[§] Florida State University.

(1) Jutzi, P. *Adv. Organomet. Chem.* **1986**, *26*, 217.
(2) (a) Panatonni, C.; Frassoon, E.; Mengegus, F. *Nature* **1963**, *199*, 1087. (b) Tyler, J. K.; Cox, A. P.; Sheridan, *Nature* **1959**, *183*, 1182. (c) Jutzi, P.; Kohl, F. X.; Krüger, C. *Angew. Chem.* **1979**, *91*, 81; *Angew. Chem., Int. Ed. Engl.* **1979**, *18*, 59. (d) Jutzi, P.; Kohl, F. X.; Hoffmann, P.; Krüger, C.; Tsay, Y.-H. *Chem. Ber.* **1980**, *113*, 757. (e) Bünder, W.; Weiss, E. *J. Organomet. Chem.* **1975**, *92*, 1. (f) Harder, S.; Prosenc, H. *Angew. Chem.* **1994**, *106*, 1830; *Angew. Chem., Int. Ed. Engl.* **1994**, *33*, 1744. (g) Atwood, J. L.; Hunter, W. E.; Cowley, A. H.; Jones, R. A.; Stewart, C. A. *J. Chem. Soc., Chem. Commun.* **1981**, 925. (h) Almenningen, A.; Haaland, A.; Motzfeldt, T. *J. Organomet. Chem.* **1967**, *7*, 97. (i) Panatonni, C.; Bombieri, G.; Croatto, *Acta Crystallogr.* **1966**, *21A*, 823. (j) Jutzi, P.; Kanne, D.; Krüger, C. *Angew. Chem.* **1986**, *98*, 163; *Angew. Chem., Int. Ed. Engl.* **1986**, *25*, 164. (k) Grenz, M.; Hahn, E.; duMont, W.-W.; Pickardt, J. *Angew. Chem.* **1984**, *96*, 69; *Angew. Chem., Int. Ed. Engl.* **1984**, *23*, 61. (l) Jutzi, P.; Wippermann, T.; Krüger, C.; Kraus, H.-J. *Angew. Chem.* **1983**, **95**, 244; *Angew. Chem., Int. Ed. Engl.* **1983**, *22*, 250. (m) Fischer, E. O.; Schreiner, S. *Chem. Ber.* **1960**, *63*, 1417.
(3) Almlof, J.; Fernholt, L.; Fægri, K., Jr.; Haaland, A.; Schilling, B. E. R.; Seip, R.; Taugbøl, *Acta Chem. Scand.* **1983**, *A37*, 131.
(4) Armstrong, D. R.; Duer, M. J.; Davidson, M. G.; Moncrieff, D.; Russell, C. A.; Stourton, C.; Steiner, A.; Stalke, D.; Wright, D. S. *Organometallics* **1997**, *16*, 3340.
(5) Dory, T. S.; Zuckerman, J. J.; Barnes, C. L. *J. Organomet. Chem.* **1985**, *281*, C1.
(6) (a) Davidson, M. G.; Stalke, D.; Wright, D. S. *Angew. Chem.* **1992**, *104*, 1265; *Angew. Chem., Int. Ed. Engl.* **1992**, *31*, 1226. (b) Edwards, A. J.; Paver, M. A.; Raithby, P. R.; Russell, C. A.; Steiner, A.; Stalke, D.; Wright, D. S. *J. Chem. Soc., Dalton Trans.* **1993**, 1465.

S0276-7333(98)00077-6 CCC: $15.00
Publication on Web 06/25/1998

tate nitrogen donors.[7] Investigation of the solid-state structures and solution dynamics of [(η-Cp)$_2$Pb·TMEDA] (**1**) (TMEDA = [Me$_2$NCH$_2$]$_2$) and [(η-Cp)$_2$Pb·4,4′-Me$_2$-bipy] (**2**) (4,4′-Me$_2$bipy = 4,4′-dimethylbipyridine) reveals that the Lewis bases are only weakly associated to the Pb(II) centers in these complexes.[7] The anomalous behavior of these species in solution has prompted us to investigate these and related Lewis-base adducts further. We present here the synthesis and structure of the new complex [(η-Cp)$_2$Sn·TMEDA] (**3**) and the investigation of the stability of the TMEDA and 4,4′-Me$_2$bipy adducts of plumbocene and stannocene by ab initio molecular orbital calculations. These studies show that steric shielding of the Sn and Pb centers in the metallocenes by the Cp ligands and the reorganization energy of the Lewis-base donor molecules prior to complexation are the major factors controlling the stability of the adducts formed. The low association energies of plumbocene and stannocene can be understood in terms of ligand lone pair/metal lone pair repulsion.

Results and Discussion

Synthesis and Structure of 3. Complex **3** was prepared in a manner similar to that for the plumbocene complexes **1** and **2**,[7] the addition of TMEDA to a solution of stannocene (1:1) in THF/toluene, giving **3** in 95% yield (Scheme 1). Despite repeated attempts to prepare the stannocene analogue of **2**, [(η-Cp)$_2$Sn·4,4′-Me$_2$bipy] (**4**), in all cases only the crystalline donor could be isolated after addition of 4,4′-Me$_2$bipy to [(η-Cp)$_2$Sn].

Scheme 1

$$[(\eta\text{-Cp})_2\text{E}] + \text{L} \xrightarrow{\text{toluene}} [(\eta\text{-Cp})_2\text{E}\cdot\text{L}]$$

E = Pb; L = TMEDA (**1**), 4,4′-Me$_2$bipy (**2**)

E = Sn; L = TMEDA (**3**)

Cryoscopic molecular mass measurements of **3** show that this complex is completely dissociated in benzene solutions over a range of concentrations ($n = 0.49 \pm 0.02$ (0.008 mol L^{-1}) and 0.49 ± 0.01 (0.022 mol L^{-1})). No splitting of the Cp resonance occurs in the ^{1}H NMR spectrum of the complex at reduced temperatures, and the ^{119}Sn NMR spectrum also consists of only a singlet regardless of the temperature ($\delta = 82.63$). The chemical shift of this resonance is almost precisely the same as that for [(η-Cp)$_2$Sn] in THF ($\delta = 82.60$). The complete dissociation of **3** into [(η-Cp)$_2$Sn] and TMEDA is in contrast to the plumbocene analogue (**1**) for which a dynamic equilibrium between the *intact* complex and [(η-Cp)$_2$Pb] and TMEDA occurs.[7] This difference in the solution dynamics of **1** and **3** is in line with the expected reduction in the Lewis acidity of Sn in stannocene, as compared to plumbocene, and with the greater development of the lone pair on the Sn center (as previously gleaned from ab initio calculations[4]). However, the complete dissociation of the 4,4′-Me$_2$bipy complex **2** in aromatic solutions as compared to only partial dissociation of the TMEDA complex **1** was an intriguing finding for which no obvious explanation is apparent, particularly in light of the solid-state structure characterization of this complex.[7] Initially, it was thought that this may simply reflect the presence of greater interaction between the 4,4′-Me$_2$bipy ligand and the aromatic solvents employed, which could encourage dissociation of **2**.[7]

Since the low-temperature X-ray structures of **1** and **2** have been reported previously,[7] no detailed discussion of their structures will be given here. Details of the structural refinement of the new complex **3** is shown in Table 1. Table 2 lists key bond lengths and angles for this complex.

The structure of **3** (Figure 1) shows features similar to those observed for **1**, the complex being monomeric

Table 1. Crystal Data for [(η-Cp)$_2$Sn·TMEDA] (3)

empirical formula	$C_{16}H_{26}N_2Sn$ **3**
fw	365.08
temp. (K)	153(2)
λ (Å)	0.710 73
cryst dimens (mm)	0.3 × 0.3 × 0.2
cryst syst	monoclinic
space group	*C*2/*c*
lattice params	
a (Å)	14.180(3)
b (Å)	9.114(2)
c (Å)	13.539(3)
β (deg)	110.97(3)
V_{cell} (Å^3)	1632.2(6)
Z	4
D_{calc} (Mg m^{-3})	1.486
μ (Mo Kα) (mm^{-1})	1.556
θ range (deg)	4.47−22.54
no. of reflns collected	1211
no. of indep reflns	945
R1 ($F > 4\sigma(F)$)[a]	0.056
wR2 (all data)	0.153
peak, hole (e Å^{-3})	2.227, −2.165

[a] R1 = $\sum|F_o - F_c|/\sum|F_o|$, wR2 = $\{[\sum w(F_o^2 - F_c^2)^2]/\sum wF_o^4\}^{0.5}$, $w = 1/[\sigma^2(F_o^2) + (xP)^2 + yP]$, $P = (F_o^2 + {}^2/_3F_c^2)$.[14]

Table 2. Selected Bond Lengths and Angles for 3

Bond Lengths (Å)			
Sn−N(1)	2.884(4)	Sn−C(4)	2.800(5)
Sn−C(1)	2.77(1)	Sn−C(5)	2.756(5)
Sn−C(2)	2.777(5)	N···N	3.046(4)
Sn−C(3)	2.817(5)	$Cp_{centroid}$−Sn	2.52

Bond Angles (deg)			
$Cp_{centroid}$−Sn−$Cp_{centroid}$	131.4	N(1)−Sn−N(1a)	64.2

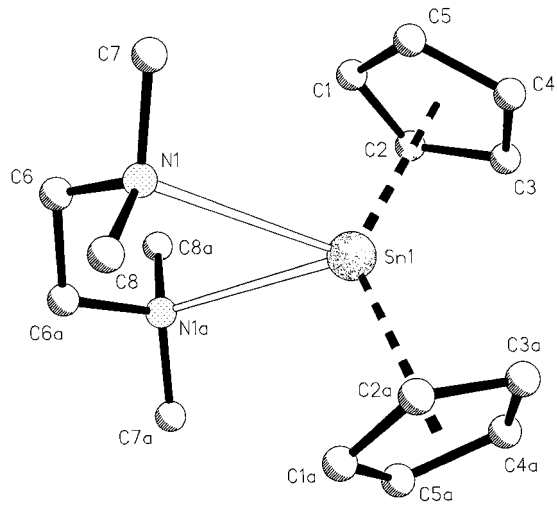

Figure 1. Structure of [(η-Cp)$_2$Sn·TMEDA] (**3**).

(7) Beswick, M. A.; Cromhout, N. L.; Harmer, C. N.; Raithby, P. R.; Russell, C. A.; Smith, J. S. B.; Steiner, A.; Wright, D. S. *J. Chem. Soc., Chem. Commun.* **1996**, 1977.

in the solid state with the Cp ligands adopting an approximately η^3-bonding mode to the metal atom. Like the plumbocene complexes (**1** and **2**), the metal−C bonds in **3** (2.77(1)−2.817(5) Å) are generally longer than those observed in the isolated metallocene (2.56(2)−2.79(2) Å in the two independent molecules of stannocene in the solid state and 2.71 Å in the gas phase)[2g,i] and the two Cp ligands adopt an eclipsed conformation (resulting in overall C_2 symmetry within the molecule). This is in contrast to the staggered arrangement found for monomeric stannocene and plumbocene in the gas phase, in which the two Cp rings are staggered with respect to each other.[2g,i] The approach of the TMEDA ligand in **3**, perpendicular to the $Cp_{centroid}-Sn-Cp_{centroid}$ axis, is hindered by the steric confrontation between the N-attached Me groups of the donor and the Cp rings. This situation results in extremely long metal−N bond lengths in **3** (Sn−N 2.884(4) Å (cf 2.24 Å estimated for the covalent bond)) as well as in **1** (Pb−N 2.879(3) Å (cf. the sum of covalent radii of N and Pb of ca. 2.28 Å)). The similarity of the metal−N bond lengths and $Cp_{centroid}-E-Cp_{centroid}$ angles in **1** and **3** ($Cp_{centroid}-E-Cp_{centroid}$ 128.8° in **1** and 131.4° in **3**[2h]) stresses the fact that the steric conflict between the approaching Lewis-base donor molecules and the Cp ligands has the primary influence over the geometries of these species. In this context, the essentially planar geometry of 4,4′-Me_2bipy leads to closer approach of this ligand and to significantly shorter metal−N distances in **2** (2.702(5) Å).

Calculational Section. In view of the apparent relative magnitudes of the metal−ligand interactions occurring in the solid-state structures of **1** and **2**, the observation that **2** undergoes complete dissociation in solution and that **1** only partially dissociates is surprising and counterintuitive. To investigate the formation and thermodynamic stabilty of these adducts, ab initio molecular orbital calculations were performed using an effective core potential (ECP) double-ζ basis set (LANL2DZ)[8] dealing with the valence electrons only for tin and lead. The other atoms were represented by Dunning−Huzinaga full double-ζ basis sets.[9] No symmetry restraints were imposed in any of these calculations. The calculations were performed using the computer program Gaussian94.[10] Table 5 shows the calculated energies for TMEDA and 4,4′-Me_2bipy. For completeness, the energies of the most stable C_{2v} eclipsed geometries of stannocene and plumbocene (determined in earlier work[4]) are also included. The optimized geometries of the most stable conformers of [(η-Cp)$_2$E] (E = Sn, Pb), TMEDA, and 4,4′-Me_2bipy are shown in Figure 2. Table 3 shows the energies of the optimized complexes [(η-Cp)$_2$Pb·TMEDA] (**1**), [(η-Cp)$_2$Pb·4,4′-Me_2bipy] (**2**), [(η-Cp)$_2$Sn·TMEDA] (**3**), and [(η-Cp)$_2$Sn·4,4′-Me_2bipy] (**4**) together with their association energies from the most stable optimized geometries of the free ligands and [(η-Cp)$_2$E]. The optimized geometries of **1**−**4** are shown in Figure 3.

Table 3. Total Energies and Association Energies of Calculated Molecules of [(η-Cp)$_2$Pb·TMEDA] (1), [(η-Cp)$_2$Pb·4,4′-Me_2bipy] (2), [(η-Cp)$_2$Sn·TMEDA] (3), and [(η-Cp)$_2$Sn·4,4′-Me_2bipy] (4)

compd	absolute energy[a]	association energy[b]
1	−732.960506	−5.90
2	−957.835739	−2.20
3	−732.840639	+0.22
4	−957.718017	+2.55

[a] In atomic units. [b] In kcal mol^{-1}.

Table 4. Total Energies of Calculated Molecules of TMEDA, 4,4′-Me_2bipy, and [(η-Cp)$_2$E] (E = Sn, Pb)

compd	total energy[a]	relative energy[b]
TMEDA (trans)	−345.263239	0.0
in **1**	−345.258207	+3.2
in **3**	−345.259286	+2.5
4,4′-Me_2bipy (trans)	−570.144331	0.0
4,4′-Me_2bipy (cis)	−570.130559	+8.6
in **2**	−570.126997	+10.9
in **4**	−570.126157	+11.4
[Cp_2Pb] (C_{2v}, eclipsed)	−387.577757	
[Cp_2Sn] (C_{2v}, eclipsed)	−387.687832	

[a] In atomic units. [b] In kcal mol^{-1}.

The optimized geometries of **1**−**4** (Figure 3) show features similar to those observed in the solid-state structures of the complexes. The only significant difference in the optimized structures occurs in the pattern of Pb−C and Sn−C distances in the TMEDA complexes **1** and **3** in which two shorter (ca. 2.886 and 2.888 Å in **1**, 2.731 and 2.740 Å in **3**) and three longer (2.900−2.916 Å in **1**, 2.856−2.946 Å in **3**) metal−C bonds are found, rather than the approximately η^3-coordination of the Cp rings observed in the crystal structures of **1** and **3**. However, in the 4,4′-Me_2bipy complexes **2** and **4**, the Cp rings adopt the anticipated η^3-mode observed experimentally in the structure of **2**. Although significantly longer than the metal−N bonds found in the crystal structures of the [(η-Cp)$_2$Pb] adducts, the variation of these distances in the calculated structures of **1** and **2** is similar, with longer metal−N bond lengths in the TMEDA complex (3.086 Å) than in the 4,4′-Me_2bipy complex (2.776 Å). This same trend is seen in the calculations involving the TMEDA and 4,4′-Me_2bipy complexes of [(η-Cp)$_2$Sn] (Sn−N 3.414 Å in **3**, Sn−N 2.562 Å in **4**).

As shown in Table 3, the calculations illustrate that the Lewis-base ligands are only loosely associated with the Pb and Sn centers of plumbocene and stannocene. The formation of the Pb complexes **1** and **2** from [(η-Cp)$_2$Pb] and TMEDA and 4,4′-Me_2bipy are favorable. However, the formation of the [(η-Cp)$_2$Sn] analogues are unfavorable (although only marginally so in the case of the TMEDA complex **3**). Despite the presence of shorter metal−ligand interactions in the Pb and Sn complexes containing 4,4′-Me_2bipy, the complexation of [(η-Cp)$_2$Pb] and [(η-Cp)$_2$Sn] by 4,4′-Me_2bipy is less favorable than by TMEDA, the association energy of **1** being 3.7 kcal mol^{-1} more favorable than **2** and that for **3** being 2.3 kcal mol^{-1} more favorable than **4**. These findings are broadly consistent with the experimental observations

(8) (a) Hay, P. J.; Wadt, W. R. *J. Chem. Phys.* **1985**, *82*, 270. (b) Wadt, W. R.; Hay, P. J. *J. Chem. Phys.* **1985**, *82*, 284. (c) Hay, P. J.; Wadt, W. R. *J. Chem. Phys.* **1985**, *82*, 299.

(9) Dunning, T. H., Jr.; Hay, P. J. In *Modern Theoretical Chemistry*; Schaefer, H. F., III, Ed.; Plenum: New York, 1976; pp 1−28.

(10) Frisch, M. J.; Trucks, G. W.; Schegel, H. B.; Gill, P. M. W.; Johnson, B. G.; Robb, M. A.; Cheeseman, J. R.; Keith, T.; Petersson, G. A.; Montgomery, J. A.; Raghavachari, K.; Al-Laham, M. A.; Zakrzewski, V. G.; Ortiz, J. V.; Foresman, J. B.; Cioslowski, J.; Stefanov, B. B.; Nonayakkara, A.; Challacombe, M.; Peng, C. Y.; Ayala, P. Y.; Chen, W.; Wong, M. W.; Andres, J. L.; Replogle, E. S.; Gompents, R.; Martin, R. L.; Fox, D.; Binkly, J. S.; Defrees, D. J.; Baker, J.; Stewart, J. J. P.; Head-Gordon, M.; Pople, J. A. Gaussian Inc.: Pittsburgh, PA, 1992.

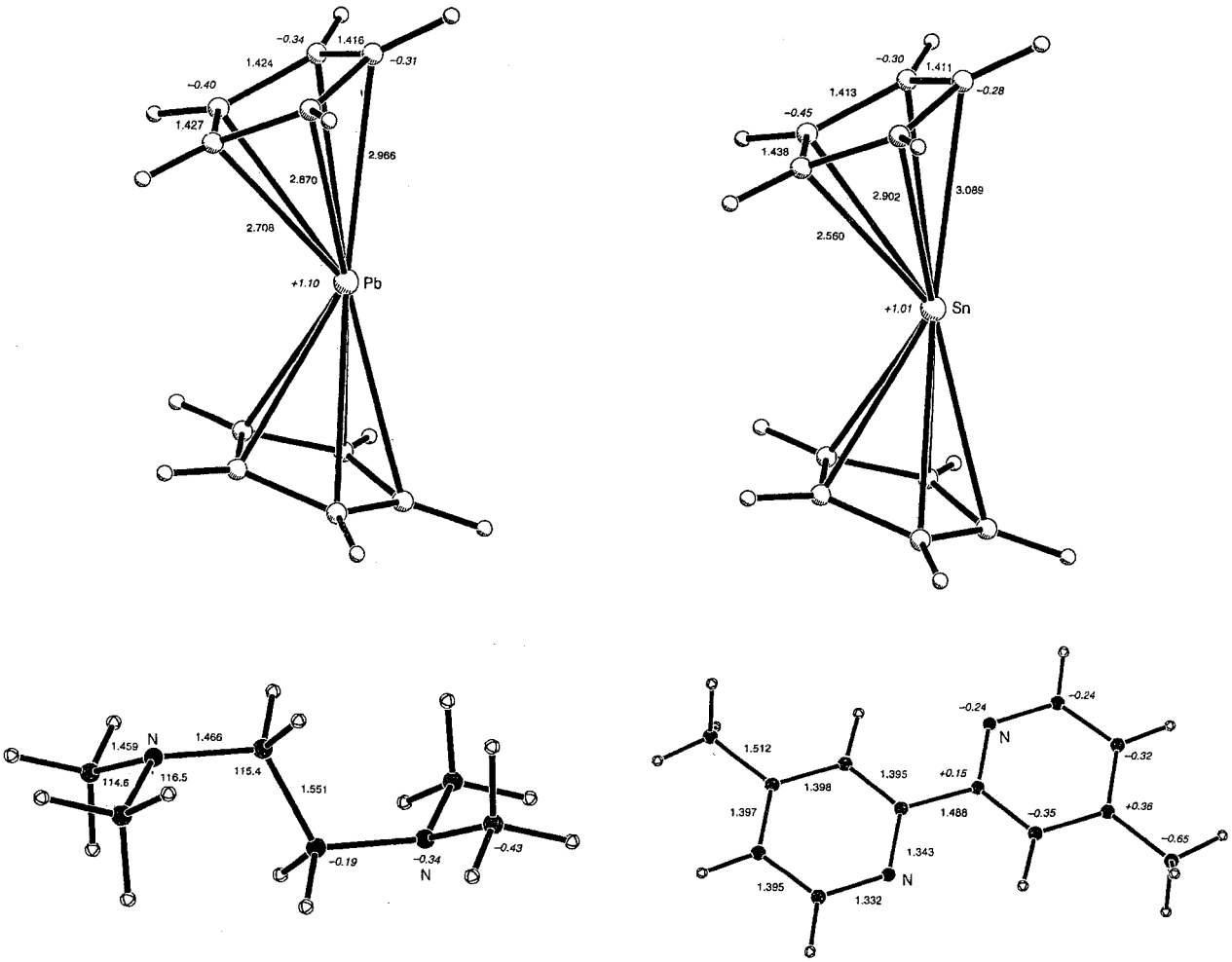

Figure 2. Ab intio optimized geometries of TMEDA, 4,4′-Me_2bipy, and [(η-Cp)$_2$E] (E = Sn, Pb), showing selected bond lengths, bond angles, and charges.

that **1** is only partially dissociated in aromatic solutions (whereas **2** and **3** are completely dissociated) and with the apparent inability of 4,4′-Me_2bipy to form an adduct with stannocene. The weakness of the bonding of the ligands to the Pb and Sn atoms in **1**−**4** is emphasized by the small electron transfer occurring from the ligands to the metals in these species, i.e., 0.10e in **2** and 0.14e in **4** from 4,4′-Me_2bipy and 0.06e in **1** and 0.04e in **3** from TMEDA. Surprisingly, the complexation of stannocene and plumbocene by TMEDA and 4,4′-Me_2bipy leads to a similar net *increase* in the charges on the metal atoms (by ca. +0.20e for both) compared to those on Sn and Pb in uncomplexed [(η-Cp)$_2$E]. Examination of the overall charge distributions in **1**−**4** shows that the small charge donated by the TMEDA and 4,4′-Me_2bipy ligands and the total charge lost by the metal centers is largely transferred to the Cp rings (the rings increasing by ca. 0.14e in **1** and **2**, 0.05e in **3** and 0.11e in **4**).

To examine why the association energies of the TMEDA complexes are greater than their 4,4′-Me_2bipy analogues, despite the shortness of the metal−ligand interaction in the latter, the energies of the TMEDA and 4,4′-Me_2bipy portions within the optimized structures of **1**−**4** were computed and compared to those for the most stable trans geometries of the isolated ligands. The results (Table 4) show that the thermodynamics of solvation of the Pb and Sn atoms of metallocenes by TMEDA and 4,4′-Me_2bipy is strongly influenced by the energies of reorganization of the ligands. This energy component is far greater for the 4,4′-Me_2bipy complexes (+10.9 kcal mol^{-1} for **2**, +11.4 kcal mol^{-1} for **4**) than for those with TMEDA (+3.2 kcal mol^{-1} for **1**, +2.5 kcal mol^{-1} for **3**). Thus, the anomolously low association energies of the 4,4′-Me_2bipy complexes are entirely due to unfavorable adjustment of the ligand within the coordination spheres of the metallocenes. Taking these energies of reorganization into account, the strengths of the metal−ligand interactions are in fact greater in the 4,4′-Me_2bipy complexes than in the TMEDA adducts, in line with the shorter metal−N bond lengths calculated for **2** and **4** and with the greater electron transfer from 4,4′-Me_2bipy to the metallocene units in these complexes. The dissociation of **2** in solution observed experimentally can be viewed as stemming from the close balance between the reorganization energy and reorganized ligand−metal association energy (+10.9 vs −13.1 kcal mol^{-1} for **2**; cf. +3.2 vs −9.1 kcal mol^{-1} for **1**).

To investigate the nature of the metal−ligand interactions in these species, a survey of the filled molecular orbitals of **1**−**4** was undertaken. It was found that in each complex there are only a small number of molecular orbitals where there is a significant contribution from both the metal and nitrogen orbitals. Basically, these molecular orbitals can be described in terms of

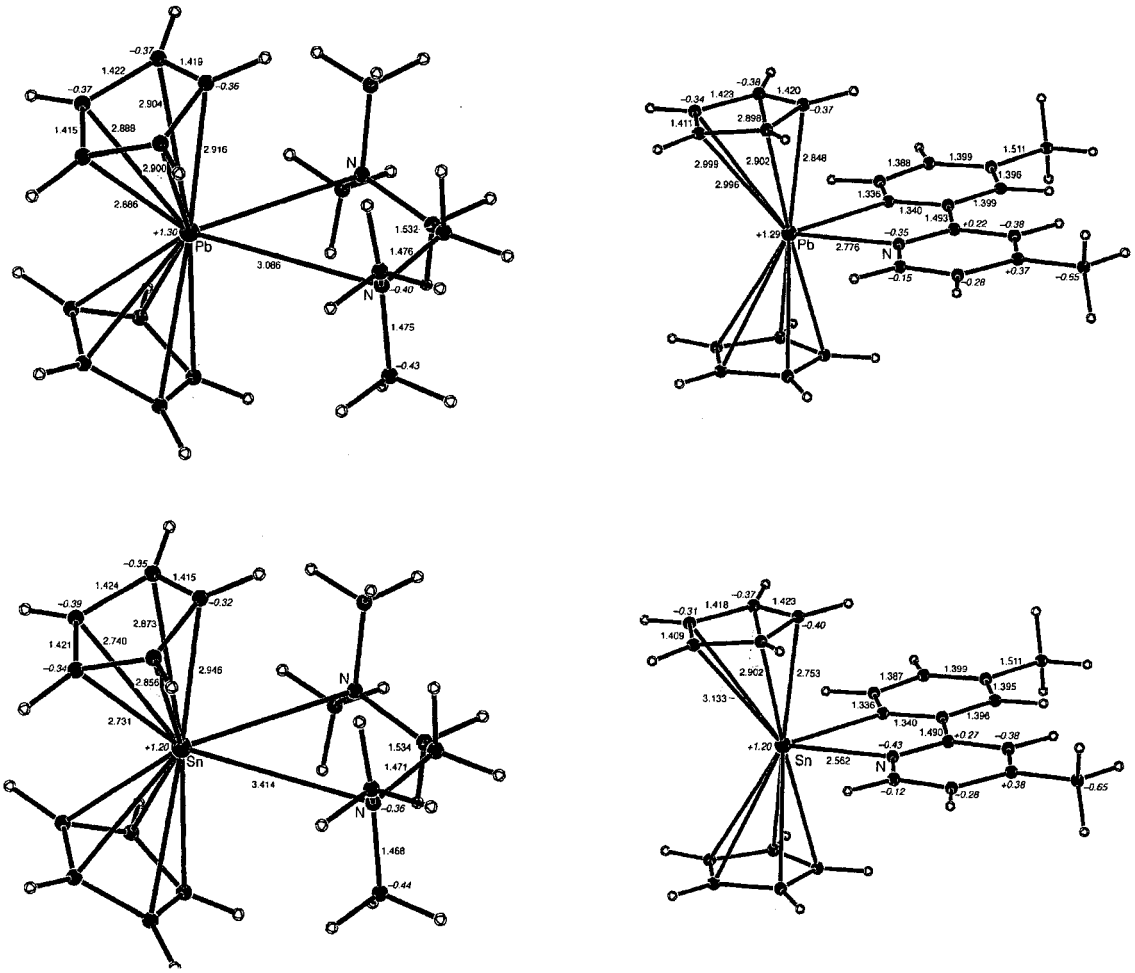

Figure 3. Ab initio optimized geometries of **1**−**4**, showing selected bond lengths, bond angles, and charges.

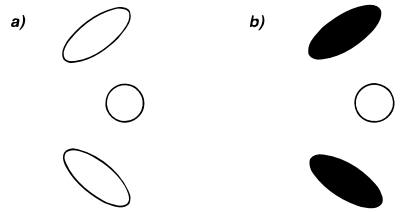

Figure 4. Schematic representations of the key molecular orbitals of [(η-Cp)$_2$E] involved in metal−ligand bonding.

the interaction of the ligand nitrogen p orbitals with the bonding and antibonding lone pair orbitals of [(η-Cp)$_2$E], which essentially correspond to the overlap of the metal s orbital with the lowest energy π molecular orbitals of the two Cp rings (Figure 4). The low association energies of [(η-Cp)$_2$E] with the reorganized TMEDA and 4,4′-Me$_2$bipy ligands can be attributed to ligand lone pair/metal lone pair repulsion. Closer scrutiny of the orbital electron populations of the metals in **1**−**4** and for the uncomplexed species [(η-Cp)$_2$E] reveals that the increase in positive charge of the metals on complexation is almost entirely due to a decrease in the population of the metal p orbital which lies along the C_{2v} axis (i.e., p_x). This orbital has traditionally been associated with the lone pair of electrons in [(η-Cp)$_2$E], and its reduced electron population suggests that complexation by the nitrogen atoms of the ligands occurs by displacement of electron density from the lone pair on the metal toward the Cp rings.

Experimental Section

General Preparative Techniques. All of the procedures were performed under dry, O$_2$-free argon using a vacuum line and standard inert-atmosphere techniques.[11] Details of the syntheses of **1** and **2** are given in ref 7.

Synthesis of 3. To a standardized solution of [(η-Cp)$_2$Sn] (6.6 mmol, 3.0 mL, 2.2 mol L^{-1} in THF) was added toluene (10 mL) and a solution of TMEDA (6.6 mmol, 1.0 mL) in toluene (10 mL). The resulting colorless solution was filtered while hot (porosity 3, Celite), and the filtrate was reduced (to ca. 10 mL) under vacuum. The precipitate formed was warmed into solution, and storage at room temperature (3 days) gave large, colorless crystalline rods of **3** (2.29 g, 95%); decomp. 125−130 °C; IR (Nujol), ν_{max} (cm^{-1}) = 3086w (C−H str, Cp−H); ^{1}H NMR (400.14 MHz, [$^2H_8$] toluene, 0.002 mol L^{-1}; 298 K: δ 5.80 (s, 10H, Cp−H), 2.21 (s, 4H, −CH$_2$−TMEDA), 2.34 (s, 12H, Me$_2$N−TMEDA). Anal. Calcd for [$C_{16}H_{26}N_2Sn$]$_n$: C, 52.6; H, 7.2; N, 7.7. Found: C, 52.9, H, 7.8, N, 7.9.

X-ray Structure Determinations. Crystals of **3** were mounted directly from solution under argon using a perfluorocarbon oil (Riedel-deHaën), which protects them from atmospheric O$_2$ and moisture.[12] The oil freezes at reduced temperatures and holds the crystal static in the X-ray beam. Data were collected on a Stoe-Siemens AED four-circle diffractometer, using graphite-monochromated Mo Kα radiation, and semiempirical absorption corrections based on ψ-scans

(11) Shriver, D. F.; Drezdon, M. A. *The Manipulation of Air-sensitive Compounds*, 2nd ed.; Wiley: New York, 1986.
(12) Stalke, D.; Kottke, T. *J. Appl. Crystallogr.*, **1993**, *26*, 615.

were employed for all complexes.[13] Details of the structural refinement of **1** are given in Table 1. The structures were solved by direct methods (SHELXTL PLUS[15]) and refined by full-matrix least squares on F^2 (SHELXL-93[14]). Atomic coordinates, bond lengths and angles, and thermal parameters for **1**−**3** have been deposited with the Cambridge Crystallography Data Centre (no. 101873).

Acknowledgment. We gratefully acknowledge the EPSRC (M.A.B., C.N.H., A.E.H.W.), the Royal Society (P.R.R., D.S.W.), The European Community (Fellowship for A.S.), Sidney Sussex College, Cambridge (Fellowship for C.A.R.), The Commonwealth Trust (N.L.C.), and the Office of Energy Research, Office of Basic Energy Sciences, Division of Chemical Sciences, U.S. Department of Energy (Grant No. DE-FG02-97ER-14758; D.M.). for financial support.

(13) Sheldrick, G. M. *XEMP, program for structure adsorption*.
(14) Sheldrick, G. M. *SHELXTL-PLUS, Structure solution and refinement package*; Siemens Analytical, Inc.: Madison, WI, 1990.
(15) Sheldrick, G. M. *SHELXL-93, structure refinement package*; University of Göttingen: Gottingen, Germany, 1993.

Supporting Information Available: Tables of crystal data and structural refinements, anisotropic and isotropic thermal parameters, full bond distances and angles, and atomic coordinates for **1**−**3** (16 pages). Ordering information is given on any current masthead page.

OM980077K